



Stress in ASME Pressure Vessels, Boilers, and Nuclear Components

Maan H. Jawad

ASME
PRESS

WILEY

**STRESS IN ASME
PRESSURE VESSELS,
BOILERS, AND NUCLEAR
COMPONENTS**

Wiley-ASME Press Series List

Stress in ASME Pressure Vessels, Boilers, and Nuclear Components	Jawad	October 2017
Robust Adaptive Control for Fractional-Order Systems with Disturbance and Saturation	Shi	November 2017
Robot Manipulator Redundancy Resolution	Zhang	October 2017
Combined Cooling, Heating, and Power Systems: Modeling, Optimization, and Operation	Shi	August 2017
Applications of Mathematical Heat Transfer and Fluid Flow Models in Engineering and Medicine	Dorfman	February 2017
Bioprocessing Piping and Equipment Design: A Companion Guide for the ASME BPE Standard	Huitt	December 2016
Nonlinear Regression Modeling for Engineering Applications	Rhinehart	September 2016
Fundamentals of Mechanical Vibrations	Cai	May 2016
Introduction to Dynamics and Control of Mechanical Engineering Systems	To	March 2016

STRESS IN ASME PRESSURE VESSELS, BOILERS, AND NUCLEAR COMPONENTS

Maan H. Jawad, Ph.D., P.E.

*Global Engineering & Technology, Inc.
Camas, WA, USA*

WILEY



This edition first published 2018
Copyright © 2018, The American Society of Mechanical Engineers (ASME), 2 Park Avenue,
New York, NY, 10016, USA (www.asme.org).
Published by John Wiley & Sons, Inc., Hoboken, New Jersey.

All rights reserved. No part of this publication may be reproduced, stored in a retrieval system, or transmitted, in any form or by any means, electronic, mechanical, photocopying, recording or otherwise, except as permitted by law. Advice on how to obtain permission to reuse material from this title is available at <http://www.wiley.com/go/permissions>.

The right of Maan H. Jawad to be identified as the author of this work has been asserted in accordance with law.

Registered Office(s)

John Wiley & Sons, Inc., 111 River Street, Hoboken, NJ 07030, USA
John Wiley & Sons Ltd, The Atrium, Southern Gate, Chichester, West Sussex, PO19 8SQ, UK

Editorial Office

The Atrium, Southern Gate, Chichester, West Sussex, PO19 8SQ, UK

For details of our global editorial offices, customer services, and more information about Wiley products visit us at www.wiley.com.

Wiley also publishes its books in a variety of electronic formats and by print-on-demand. Some content that appears in standard print versions of this book may not be available in other formats.

Limit of Liability/Disclaimer of Warranty

While the publisher and authors have used their best efforts in preparing this work, they make no representations or warranties with respect to the accuracy or completeness of the contents of this work and specifically disclaim all warranties, including without limitation any implied warranties of merchantability or fitness for a particular purpose. No warranty may be created or extended by sales representatives, written sales materials or promotional statements for this work. The fact that an organization, website, or product is referred to in this work as a citation and/or potential source of further information does not mean that the publisher and authors endorse the information or services the organization, website, or product may provide or recommendations it may make. This work is sold with the understanding that the publisher is not engaged in rendering professional services. The advice and strategies contained herein may not be suitable for your situation. You should consult with a specialist where appropriate. Further, readers should be aware that websites listed in this work may have changed or disappeared between when this work was written and when it is read. Neither the publisher nor authors shall be liable for any loss of profit or any other commercial damages, including but not limited to special, incidental, consequential, or other damages.

Library of Congress Cataloging-in-Publication Data

Names: Jawad, Maan H., author.

Title: Stress in ASME pressure vessels, boilers and nuclear components / by
Maan H. Jawad.

Description: First edition. | Hoboken, NJ : John Wiley & Sons, 2018. |

Series: Wiley-ASME Press series | Includes bibliographical references and index. |

Identifiers: LCCN 2017018768 (print) | LCCN 2017036797 (ebook) | ISBN

9781119259268 (pdf) | ISBN 9781119259275 (epub) | ISBN 9781119259282 (cloth)

Subjects: LCSH: Shells (Engineering) | Plates (Engineering) | Strains and stresses.

Classification: LCC TA660.S5 (ebook) | LCC TA660.S5 J39 2017 (print) | DDC
624.1/776–dc23

LC record available at <https://lccn.loc.gov/2017018768>

Cover design by Wiley

Cover image: © I Verveer/Gettyimages

Set in 10/12pt Times by SPi Global, Pondicherry, India

Contents

Series Preface	ix
Acknowledgment	xi
1 Membrane Theory of Shells of Revolution	1
1.1 Introduction	1
1.2 Basic Equations of Equilibrium	1
1.3 Spherical and Ellipsoidal Shells Subjected to Axisymmetric Loads	6
1.4 Conical Shells	18
1.5 Cylindrical Shells	20
1.6 Cylindrical Shells with Elliptical Cross Section	22
1.7 Design of Shells of Revolution	23
Problems	23
2 Various Applications of the Membrane Theory	27
2.1 Analysis of Multicomponent Structures	27
2.2 Pressure–Area Method of Analysis	35
2.3 Deflection Due to Axisymmetric Loads	42
Problems	47
3 Analysis of Cylindrical Shells	51
3.1 Elastic Analysis of Thick-Wall Cylinders	51
3.2 Thick Cylinders with Off-center Bore	56
3.3 Stress Categories and Equivalent Stress Limits for Design and Operating Conditions	57
3.4 Plastic Analysis of Thick Wall Cylinders	63
3.5 Creep Analysis of Thick-Wall Cylinders	65
3.6 Shell Equations in the ASME Code	69
3.7 Bending of Thin-Wall Cylinders Due to Axisymmetric Loads	71

3.8	Thermal Stress	89
3.9	Discontinuity Stresses	98
	Problems	100
4	Buckling of Cylindrical Shells	103
4.1	Introduction	103
4.2	Basic Equations	103
4.3	Lateral Pressure	108
4.4	Lateral and End Pressure	114
4.5	Axial Compression	117
4.6	Design Equations	120
	Problems	136
5	Stress in Shells of Revolution Due to Axisymmetric Loads	141
5.1	Elastic Stress in Thick-Wall Spherical Sections Due to Pressure	141
5.2	Spherical Shells in the ASME Code	142
5.3	Stress in Ellipsoidal Shells Due to Pressure Using Elastic Analysis	145
5.4	Ellipsoidal (Dished) Heads in the ASME Code	146
5.5	Stress in Thick-Wall Spherical Sections Due to Pressure Using Plastic Analysis	150
5.6	Stress in Thick-Wall Spherical Sections Due to Pressure Using Creep Analysis	150
5.7	Bending of Shells of Revolution Due to Axisymmetric Loads	151
5.8	Spherical Shells	156
5.9	Conical Shells	165
	Problems	174
6	Buckling of Shells of Revolution	175
6.1	Elastic Buckling of Spherical Shells	175
6.2	ASME Procedure for External Pressure	179
6.3	Buckling of Stiffened Spherical Shells	180
6.4	Ellipsoidal Shells	181
6.5	Buckling of Conical Shells	181
6.6	Various Shapes	184
	Problems	184
7	Bending of Rectangular Plates	187
7.1	Introduction	187
7.2	Strain–Deflection Equations	189
7.3	Stress–Deflection Expressions	194
7.4	Force–Stress Expressions	196
7.5	Governing Differential Equations	197
7.6	Boundary Conditions	200

7.7	Double Series Solution of Simply Supported Plates	204
7.8	Single Series Solution of Simply Supported Plates	206
7.9	Rectangular Plates with Fixed Edges	211
7.10	Plate Equations in the ASME Code	212
	Problems	213
8	Bending of Circular Plates	215
8.1	Plates Subjected to Uniform Loads in the θ -Direction	215
8.2	Circular Plates in the ASME Code	225
8.3	Plates on an Elastic Foundation	227
8.4	Plates with Variable Boundary Conditions	231
8.5	Design of Circular Plates	234
	Problems	235
9	Approximate Analysis of Plates	239
9.1	Introduction	239
9.2	Yield Line Theory	239
9.3	Further Application of the Yield Line Theory	247
9.4	Design Concepts	253
	Problems	255
10	Buckling of Plates	259
10.1	Circular Plates	259
10.2	Rectangular Plates	263
10.3	Rectangular Plates with Various Boundary Conditions	271
10.4	Finite Difference Equations for Buckling	275
10.5	Other Aspects of Buckling	277
10.6	Application of Buckling Expressions to Design Problems	279
	Problems	282
11	Finite Element Analysis	283
11.1	Definitions	283
11.2	One-Dimensional Elements	287
11.3	Linear Triangular Elements	295
11.4	Axisymmetric Triangular Linear Elements	302
11.5	Higher-Order Elements	305
11.6	Nonlinear Analysis	307
Appendix A:	Fourier Series	309
A.1	General Equations	309
A.2	Interval Change	313
A.3	Half-Range Expansions	314
A.4	Double Fourier Series	316

Appendix B: Bessel Functions	319
B.1 General Equations	319
B.2 Some Bessel Identities	323
B.3 Simplified Bessel Functions	325
Appendix C: Conversion Factors	327
References	329
Answers to Selected Problems	333
Index	335

Series Preface

The *Wiley-ASME Press Series in Mechanical Engineering* brings together two established leaders in mechanical engineering publishing to deliver high-quality, peer-reviewed books covering topics of current interest to engineers and researchers worldwide. The series publishes across the breadth of mechanical engineering, comprising research, design and development, and manufacturing. It includes monographs, references, and course texts. Prospective topics include emerging and advanced technologies in engineering design, computer-aided design, energy conversion and resources, heat transfer, manufacturing and processing, systems and devices, renewable energy, robotics, and biotechnology.

Acknowledgment

The author would like to thank Mr. Donald Lange of the CIC Group and Bernard Wicklein and Grace Fechter of the Nooter Corporation in St. Louis, Missouri, for their support. Special thanks are also given to Dr Chithranjan Nadarajah for providing the finite element analysis of the quadratic element in Chapter 11.

1

Membrane Theory of Shells of Revolution

1.1 Introduction

All thin cylindrical shells, spherical and ellipsoidal heads, and conical transition sections are generally analyzed and designed in accordance with the general membrane theory of shells of revolution. These components include those designed in accordance with the ASME pressure vessel code (Section VIII), boiler code (Section I), and nuclear code (Section III). Some adjustments are sometimes made to the calculated thicknesses when the ratio of radius to thickness is small or when other factors such as creep or plastic analysis enter into consideration. The effect of these factors is discussed in later chapters, whereas assumptions and derivation of the basic membrane equations needed to analyze shells of revolution due to various loading conditions are described here.

1.2 Basic Equations of Equilibrium

The membrane shell theory is used extensively in designing such structures as flat bottom tanks, pressure vessel components (Figure 1.1), and vessel heads. The membrane theory assumes that equilibrium in the shell is achieved by having the in-plane membrane forces resist all applied loads without any bending moments. The theory gives accurate results as long as the applied loads are distributed over a large area of the shell such as pressure and wind loads. The membrane forces by themselves cannot resist local concentrated loads. Bending moments are needed to resist such loads as discussed in Chapters 3 and 5. The basic assumptions made in deriving the membrane theory (Gibson 1965) are as follows:

1. The shell is homogeneous and isotropic.
2. The thickness of the shell is small compared with its radius of curvature.



Figure 1.1 Pressure vessels. Source: Courtesy of the Nooter Corporation, St. Louis, MO.

3. The bending strains are negligible and only strains in the middle surface are considered.
4. The deflection of the shell due to applied loads is small.

In order to derive the governing equations for the membrane theory of shells, we need to define the shell geometry. The middle surface of a shell of constant thickness may be considered a surface of revolution. A surface of revolution is obtained by rotating a plane curve about an axis lying in the plane of the curve. This curve is called a meridian (Figure 1.2). Any point in the middle surface can be described first by specifying the meridian on which it is located and second by specifying a quantity, called a parallel circle, that varies along the meridian and is constant on a circle around the axis of the shell. The meridian is defined by the angle θ and the parallel circle by ϕ as shown in Figure 1.2.

Define r (Figure 1.3) as the radius from the axis of rotation to any given point o on the surface; r_1 as the radius from point o to the center of curvature of the meridian; and r_2 as the radius from the axis of revolution to point o , and it is perpendicular to the meridian. Then from Figure 1.3,

$$r = r_2 \sin \phi, \quad ds = r_1 d\phi, \quad \text{and} \quad dr = r_2 \cos \phi. \quad (1.1)$$

The interaction between the applied loads and resultant membrane forces is obtained from statics and is shown in Figure 1.4. Shell forces N_ϕ and N_θ are membrane forces in the meridional

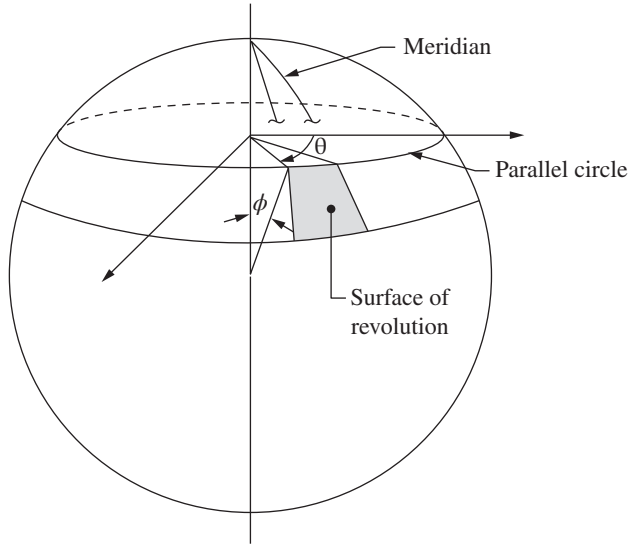


Figure 1.2 Surface of revolution

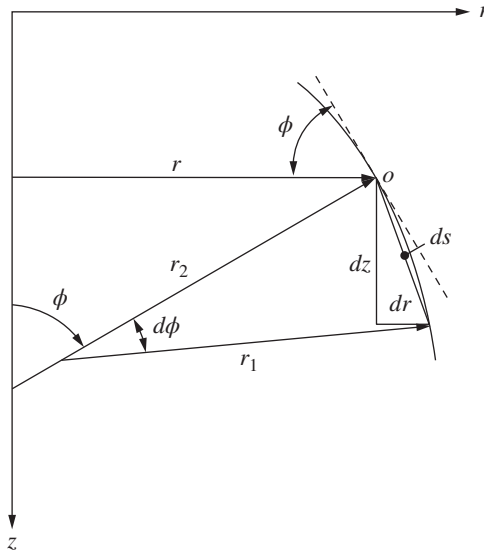


Figure 1.3 Shell geometry

and circumferential directions, respectively. Shearing forces $N_{\phi\theta}$ and $N_{\theta\phi}$ are as shown in Figure 1.4. Applied load p_r is perpendicular to the surface of the shell, load p_ϕ is in the meridional direction, and load p_θ is in the circumferential direction. All forces are positive as shown in Figure 1.4.

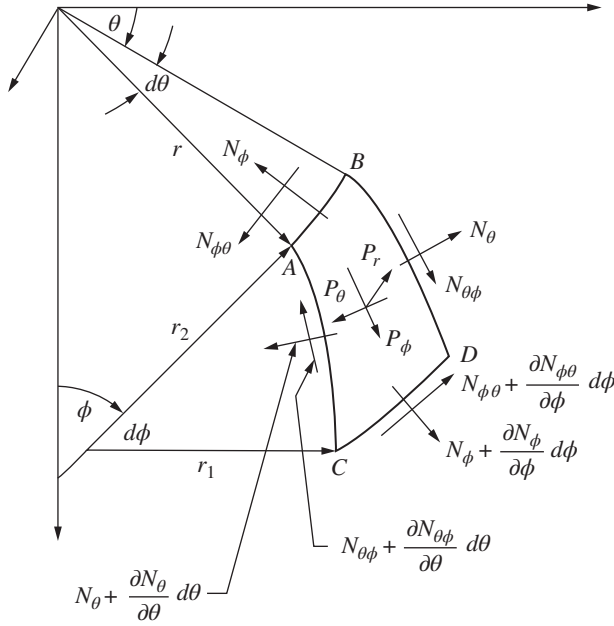


Figure 1.4 Membrane forces and applied loads

The first equation of equilibrium is obtained by summing forces parallel to the tangent at the meridian. This yields

$$\begin{aligned}
 N_{\theta\phi}r_1d\phi - \left(N_{\theta\phi} + \frac{\partial N_{\theta\phi}}{\partial\theta}d\theta\right)r_1d\phi - N_{\phi}r d\theta \\
 + \left(N_{\phi} + \frac{\partial N_{\phi}}{\partial\phi}d\phi\right)\left(r + \frac{\partial r}{\partial\phi}d\phi\right)d\theta \\
 + p_{\phi}r d\theta r_1d\phi - N_{\theta}r_1d\phi d\theta \cos\phi = 0.
 \end{aligned} \tag{1.2}$$

The last term in Eq. (1.2) is the component of N_{θ} parallel to the tangent at the meridian (Jawad 2004). It is obtained from Figure 1.5. Simplifying Eq. (1.2) and neglecting terms of higher order results in

$$\frac{\partial}{\partial\phi}(rN_{\phi}) - r_1\frac{\partial N_{\theta\phi}}{\partial\theta} - r_1N_{\theta}\cos\phi + p_{\phi}rr_1 = 0. \tag{1.3}$$

The second equation of equilibrium is obtained from summation of forces in the direction of parallel circles. Referring to Figure 1.4,

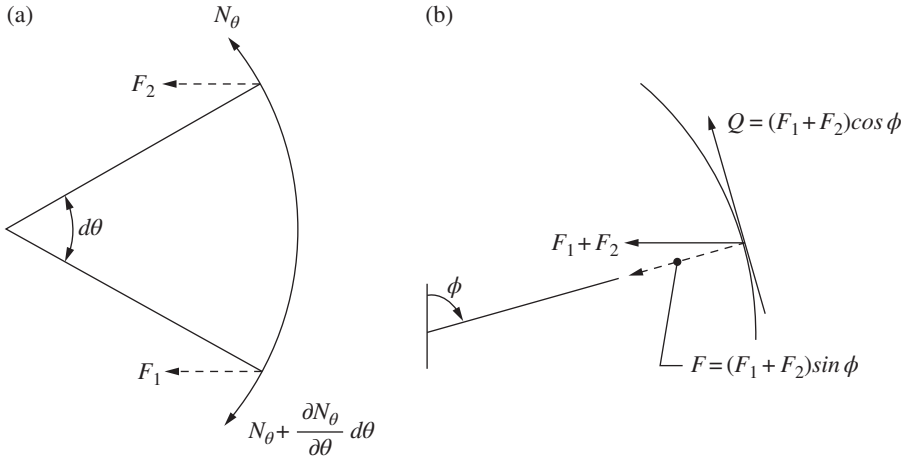


Figure 1.5 Components of N_θ : (a) circumferential cross section and (b) longitudinal cross section

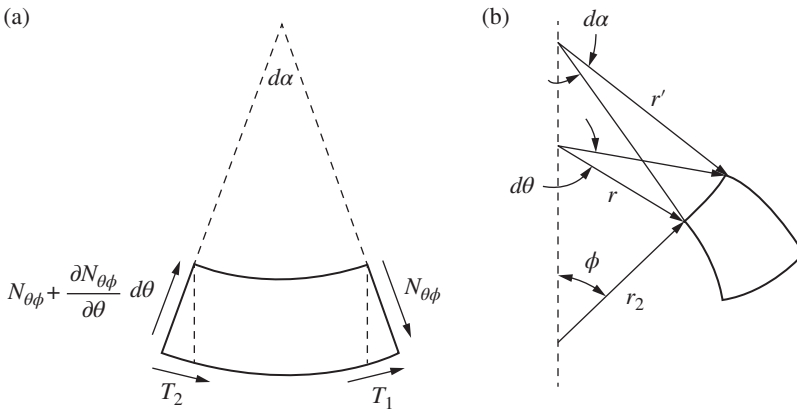


Figure 1.6 Components of $N_{\theta\phi}$: (a) side view and (b) three-dimensional view

$$\begin{aligned}
 & N_{\phi\theta}r d\theta - \left(N_{\phi\theta} + \frac{\partial N_{\phi\theta}}{\partial\phi} d\phi \right) \left(r + \frac{\partial r}{\partial\phi} d\phi \right) d\theta \\
 & - N_{\theta}r_1 d\phi + \left(N_{\theta} + \frac{\partial N_{\theta}}{\partial\theta} d\theta \right) (r_1 d\phi) \\
 & + p_{\theta}r d\theta r_1 d\phi - N_{\theta\phi}r_1 d\phi \frac{\cos\phi d\theta}{2} \\
 & - \left(N_{\theta\phi} + \frac{\partial N_{\theta\phi}}{\partial\theta} d\theta \right) (r_1 d\phi) \frac{\cos\phi d\theta}{2} = 0.
 \end{aligned} \tag{1.4}$$

The last two expressions in this equation are obtained from Figure 1.6 (Jawad 2004) and are the components of $N_{\theta\phi}$ in the direction of the parallel circles. Simplifying this equation results in

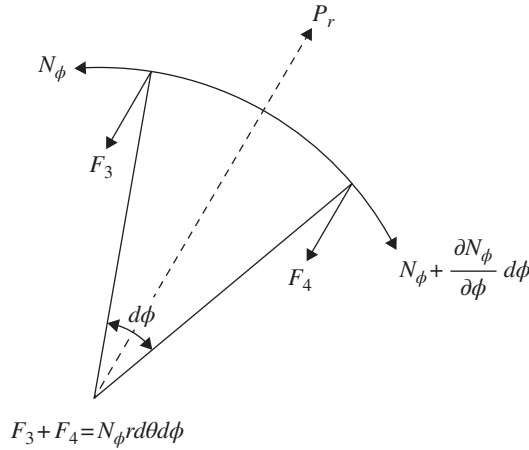


Figure 1.7 Components of N_ϕ

$$\frac{\partial}{\partial \phi} (rN_{\phi\theta}) - r_1 \frac{\partial N_\theta}{\partial \theta} + r_1 N_{\theta\phi} \cos \phi - p_\theta r r_1 = 0. \quad (1.5)$$

This is the second equation of equilibrium of the infinitesimal element shown in Figure 1.4. The last equation of equilibrium is obtained by summing forces perpendicular to the middle surface. Referring to Figures 1.4, 1.5, and 1.7,

$$(N_\theta r_1 d\phi d\theta) \sin \phi - p_r r d\theta r_1 d\phi + N_\phi r d\theta d\phi = 0$$

or

$$N_\theta r_1 \sin \phi + N_\phi r = p_r r r_1. \quad (1.6)$$

Equations (1.3), (1.5), and (1.6) are the three equations of equilibrium of a shell of revolution subjected to axisymmetric loads.

1.3 Spherical and Ellipsoidal Shells Subjected to Axisymmetric Loads

In many structural applications, loads such as deadweight, snow, and pressure are symmetric around the axis of the shell. Hence, all forces and deformations must also be symmetric around the axis. Accordingly, all loads and forces are independent of θ and all derivatives with respect to θ are zero. Equation (1.3) reduces to

$$\frac{\partial}{\partial \phi} (rN_\phi) - r_1 N_\theta \cos \phi = -p_\phi r r_1. \quad (1.7)$$

Equation (1.5) becomes

$$\frac{\partial}{\partial \phi} (rN_{\theta\phi}) + r_1 N_{\theta\phi} \cos \phi = p_{\theta} r r_1. \quad (1.8)$$

In this equation, we let the cross shears $N_{\phi\theta} = N_{\theta\phi}$ in order to maintain equilibrium.

Equation (1.6) can be expressed as

$$\frac{N_{\theta}}{r_2} + \frac{N_{\phi}}{r_1} = p_r. \quad (1.9)$$

Equation (1.8) describes a torsion condition in the shell. This condition produces deformations around the axis of the shell. However, the deformation around the axis is zero due to axisymmetric loads. Hence, we must set $N_{\theta\phi} = p_{\theta} = 0$ and we disregard Eq. (1.8) from further consideration.

Substituting Eq. (1.9) into Eq. (1.7) gives

$$N_{\phi} = \frac{1}{r_2 \sin^2 \phi} \left[\int r_1 r_2 (p_r \cos \phi - p_{\phi} \sin \phi) \sin \phi d\phi + C \right]. \quad (1.10)$$

The constant of integration C in Eq. (1.10) is additionally used to take into consideration the effect of any additional applied loads that cannot be defined by p_r and p_{ϕ} such as weight of contents.

Equations (1.9) and (1.10) are the two governing equations for designing double-curvature shells under membrane action.

1.3.1 Spherical Shells Subjected to Internal Pressure

For spherical shells under axisymmetric loads, the differential equations can be simplified by letting $r_1 = r_2 = R$. Equations (1.9) and (1.10) become

$$N_{\phi} + N_{\theta} = p_r R \quad (1.11)$$

and

$$N_{\phi} = \frac{R}{\sin^2 \phi} \left[\int (p_r \cos \phi - p_{\phi} \sin \phi) \sin \phi d\phi + C \right]. \quad (1.12)$$

These two expressions form the basis for developing solutions to various loading conditions in spherical shells. For any loading condition, expressions for p_r and p_{ϕ} are first determined and then the previous equations are solved for N_{ϕ} and N_{θ} .

For a spherical shell under internal pressure, $p_r = P$ and $p_{\phi} = 0$. Hence, from Eqs. (1.11) and (1.12),

$$N_{\phi} = N_{\theta} = \frac{PR}{2} = \frac{PD}{4} \quad (1.13)$$

where D is the diameter of the sphere. The required thickness is obtained from

$$t = \frac{N_\phi}{S} = \frac{N_\theta}{S} \quad (1.14)$$

where S is the allowable stress.

Equation (1.14) is accurate for design purposes as long as $R/t \geq 10$. If $R/t < 10$, then thick shell equations, described in Chapter 3, must be used.

1.3.2 Spherical Shells under Various Loading Conditions

The following examples illustrate the use of Eqs. (1.11) and (1.12) for determining forces in spherical segments subjected to various loading conditions.

Example 1.1

A storage tank roof with thickness t has a dead load of γ psf. Find the expressions for N_ϕ and N_θ .

Solution

From Figure 1.8a and Eq. (1.12),

$$\begin{aligned} p_r &= -\gamma \cos \phi \quad \text{and} \quad p_\phi = \gamma \sin \phi \\ N_\phi &= \frac{R}{\sin^2 \phi} \left[\int (-\gamma \cos^2 \phi - \gamma \sin^2 \phi) \sin \phi d\phi + C \right] \\ N_\phi &= \frac{R}{\sin^2 \phi} (\gamma \cos \phi + C). \end{aligned} \quad (1)$$

As ϕ approaches zero, the denominator in Eq. (1) approaches zero. Accordingly, we must let the bracketed term in the numerator equal zero. This yields $C = -\gamma$. Equation (1) becomes

$$N_\phi = \frac{-R\gamma(1 - \cos \phi)}{\sin^2 \phi}. \quad (2)$$

The convergence of Eq. (2) as ϕ approaches zero can be checked by l'Hopital's rule. Thus,

$$N_\phi \Big|_{\phi=0} = \frac{-R\gamma \sin \phi}{2 \sin \phi \cos \phi} \Big|_{\phi=0} = \frac{-\gamma R}{2}.$$

Equation (2) can be written as

$$N_\phi = \frac{-\gamma R}{1 + \cos \phi}. \quad (3)$$

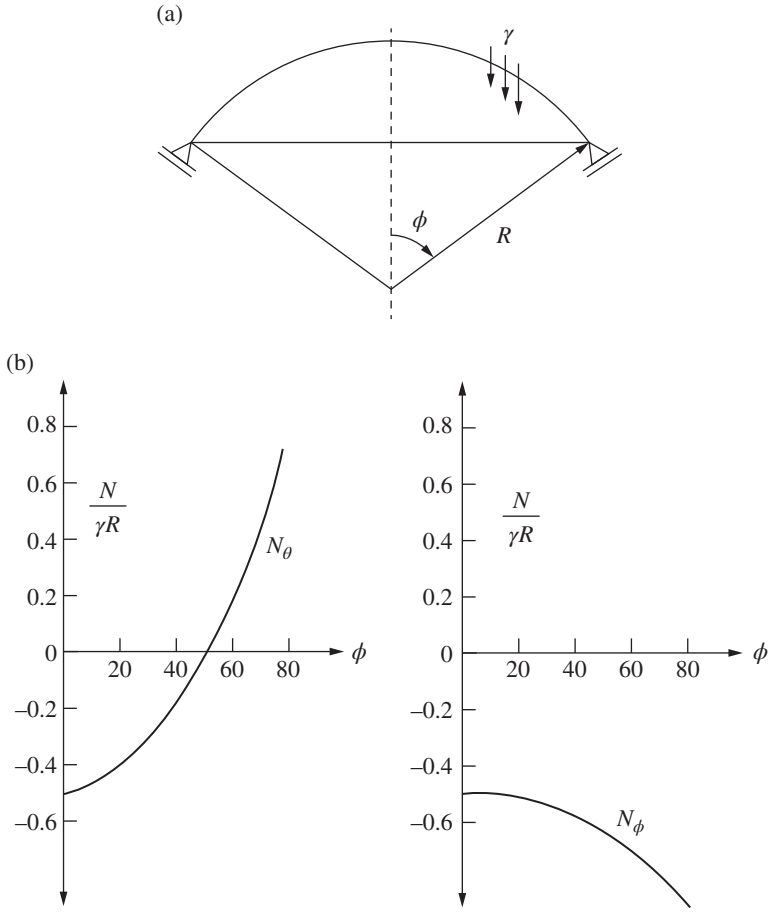


Figure 1.8 Membrane forces in a head due to deadweight: (a) dead load and (b) force patterns

From Eq. (1.11), N_θ is given by

$$N_\theta = \gamma R \left(\frac{1}{1 + \cos \phi} - \cos \phi \right). \tag{4}$$

A plot of N_ϕ and N_θ for various values of ϕ is shown in Figure 1.8b, showing that for angles ϕ greater than 52° , the hoop force, N_θ , changes from compression to tension and special attention is needed in using the appropriate allowable stress values.

Example 1.2

Find the forces in a spherical head due to a vertical load P_o applied at an angle $\phi = \phi_o$ as shown in Figure 1.9a.

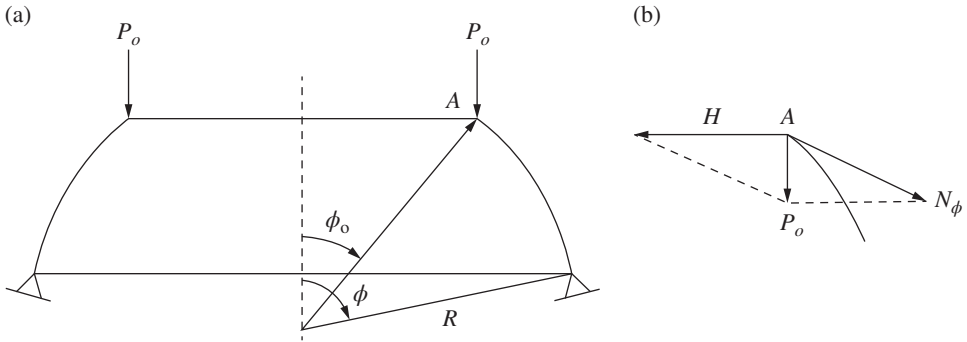


Figure 1.9 Edge loads in a spherical head: (a) edge load and (b) forces due to edge load

Solution

Since $p_r = p_\phi = 0$, Eq. (1.12) becomes

$$N_\phi = \frac{RC}{\sin^2 \phi}. \quad (1)$$

From statics at $\phi = \phi_o$, we get from Figure 1.9b

$$N_\phi = \frac{P_o}{\sin \phi_o}.$$

Substituting this expression into Eq. (1), and keeping in mind that it is a compressive membrane force, gives

$$C = \frac{-P_o}{R} \sin \phi_o$$

and Eq. (1) yields

$$N_\phi = -P_o \frac{\sin \phi_o}{\sin^2 \phi}.$$

From Eq. (1.11),

$$N_\theta = P_o \frac{\sin \phi_o}{\sin \phi}.$$

In this example there is another force that requires consideration. Referring to Figure 1.9b, it is seen that in order for P_o and N_ϕ to be in equilibrium, another horizontal force, H , must be considered. The direction of H is inward in order for the force system to have a net resultant force P_o downward. This horizontal force is calculated as

$$H = \frac{-P_o \cos \phi_o}{\sin \phi_o}.$$

A compression ring is needed at the inner edge in order to contain force H . The required area, A , of the ring is given by

$$A = \frac{H(R \sin \phi_o)}{\sigma}$$

where σ is the allowable compressive stress of the ring.

Example 1.3

The sphere shown in Figure 1.10a is filled with a liquid of density γ . Hence, p_r and p_ϕ can be expressed as

$$p_r = \gamma R(1 - \cos \phi)$$

$$p_\phi = 0.$$

- a. Determine the expressions for N_ϕ and N_θ throughout the sphere.
- b. Plot N_ϕ and N_θ for various values of ϕ when $\phi_o = 110^\circ$.
- c. Plot N_ϕ and N_θ for various values of ϕ when $\phi_o = 130^\circ$.
- d. If $\gamma = 62.4$ pcf, $R = 30$ ft, and $\phi_o = 110^\circ$, determine the magnitude of the unbalanced force H at the cylindrical shell junction. Design the sphere, the support cylinder, and the junction ring. Let the allowable stress in tension be 20 ksi and that in compression be 10 ksi.

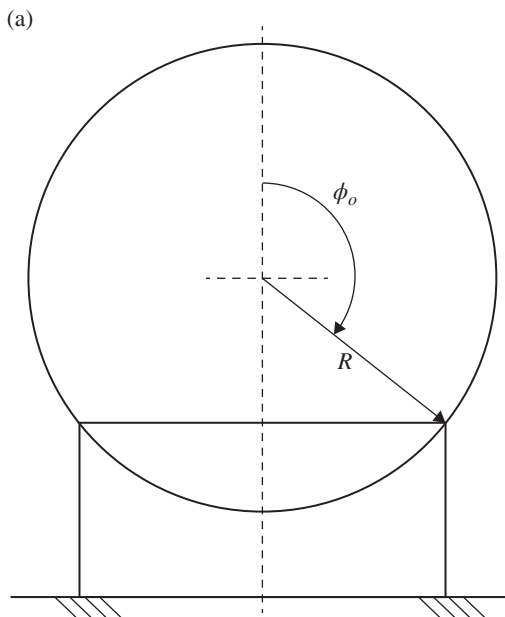


Figure 1.10 Spherical tank: (a) spherical tank, (b) support at 110° , (c) support at 130° , and (d) forces at support junction

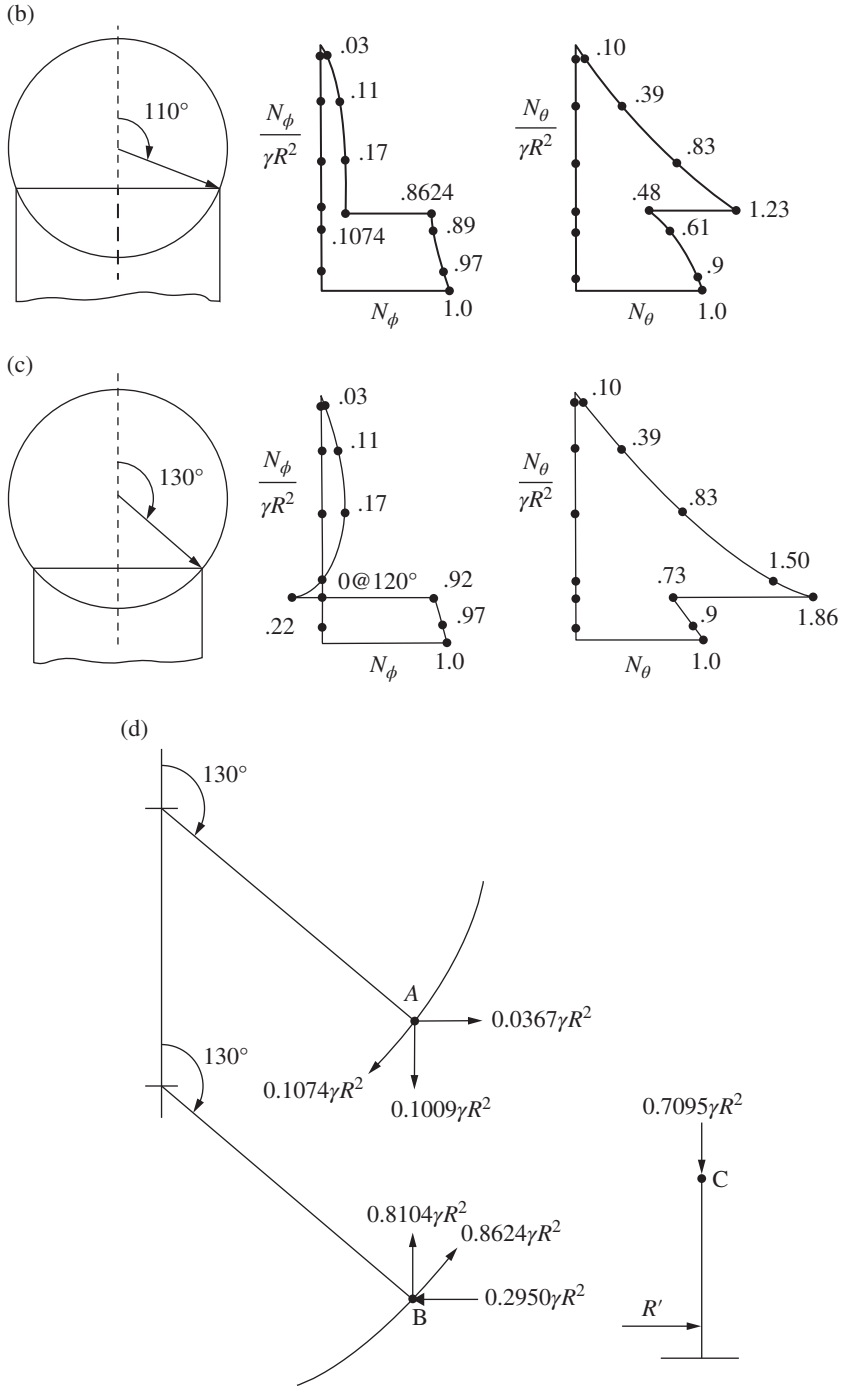


Figure 1.10 (Continued)

Solution

a. From Eq. (1.12), we obtain

$$N_\phi = \frac{\gamma R^2}{\sin^2 \phi} \left(\frac{1}{2} \sin^2 \phi + \frac{1}{3} \cos^3 \phi + C \right). \quad (1)$$

As ϕ approaches zero, the denominator approaches zero. Hence, the bracketed term in the numerator must be set to zero. This gives $C = -1/3$ and Eq. (1) becomes

$$N_\phi = \frac{\gamma R^2}{6 \sin^2 \phi} (3 \sin^2 \phi + 2 \cos^3 \phi - 2). \quad (2)$$

The corresponding N_θ from Eq. (1.11) is

$$N_\theta = \gamma R^2 \left[\frac{1}{2} - \cos \phi - \frac{1}{3 \sin^2 \phi} (\cos^3 \phi - 1) \right]. \quad (3)$$

As ϕ approaches π , we need to evaluate Eq. (1) at that point to ensure a finite solution. Again the denominator approaches zero and the bracketed term in the numerator must be set to zero. This gives $C = 1/3$ and Eq. (1) becomes

$$N_\phi = \frac{\gamma R^2}{6 \sin^2 \phi} (3 \sin^2 \phi + 2 \cos^3 \phi + 2). \quad (4)$$

The corresponding N_θ from Eq. (1.11) is

$$N_\theta = \gamma R^2 \left[\frac{1}{2} - \cos \phi - \frac{1}{3 \sin^2 \phi} (\cos^3 \phi + 1) \right]. \quad (5)$$

Equations (2) and (3) are applicable between $0 < \phi < \phi_o$, and Eqs. (4) and (5) are applicable between $\phi_o < \phi < \pi$.

- b. A plot of Eqs. (2) through (5) for $\phi_o = 110^\circ$ is shown in Figure 1.10b. N_ϕ below circle $\phi_o = 110^\circ$ is substantially larger than that above circle 110° . This is due to the fact that most of the weight of the contents is supported by the spherical portion that is below the circle $\phi_o = 110^\circ$. Also, because N_ϕ does not increase in proportion to the increase in pressure as ϕ increases, Eq. (1.11) necessitates a rapid increase in N_θ in order to maintain the relationship between the left- and right-hand sides. This is illustrated in Figure 1.10b.

A plot of N_ϕ and N_θ for $\phi_o = 130^\circ$ is shown in Figure 1.10c. In this case, N_ϕ is in compression just above the circle $\phi_o = 130^\circ$. This indicates that as the diameter of the supporting cylinder gets smaller, the weight of the water above circle $\phi_o = 130^\circ$ must be supported by the sphere in compression. This results in a much larger N_θ value just above $\phi_o = 130^\circ$. Buckling of the sphere becomes a consideration in this case.

- c. From Figure 1.10b for $\phi_o = 110^\circ$, the maximum force in the sphere is $N_\theta = 1.23\gamma R^2$. The required thickness of the sphere is

$$t = \frac{1.23(62.4)(30)^2/12}{20,000}$$

$$= 0.29 \text{ inch.}$$

A free-body diagram of the spherical and cylindrical junction at $\phi_o = 110^\circ$ is shown in Figure 1.10d. The values of N_ϕ at points A and B are obtained from Eqs. (2) and (4), respectively. The vertical and horizontal components of these forces are shown at points A and B in Figure 1.10d. The unbalanced vertical forces result in a downward force at point C of magnitude $0.7095\gamma R^2$. The total force on the cylinder is $(0.7095\gamma R^2)(2\pi)(R)(\sin(180 - 110))$. This total force is equal to the total weight of the contents in the sphere given by $(4/3)(\pi R^3)\gamma$. The required thickness of the cylinder is

$$t = \frac{0.7095(62.4)(30)^2/12}{10,000}$$

$$= 0.33 \text{ inch.}$$

Summation of horizontal forces at points A and B results in a compressive force of magnitude $0.2583\gamma R^2$. The needed area of compression ring at the cylinder to sphere junction is

$$A = \frac{Hr}{\sigma} = \frac{0.2583 \times 62.4 \times 30^2 (30 \sin 70)}{10,000}$$

$$= 40.89 \text{ inch}^2.$$

This area is furnished by a large ring added to the sphere or an increase in the thickness of the sphere at the junction.

1.3.3 ASME Code Equations for Spherical Shells under Various Loading Conditions

Loading conditions such as those shown in Examples 1.1 through 1.3 are not specifically covered by equations in the boiler and pressure vessel codes. However, they are addressed in paragraph PG-16.1 of Section I, paragraph U-2(g) of Section VIII-1, and paragraph 4.1.1 of Section VIII-2 using special analysis.

In the nuclear code, paragraph NC-3932.2 of Section NC and ND-3932.2 of Section ND provide equations for calculating forces at specific locations in a shell due to loading conditions similar to those shown in Examples 1.1 through 1.5. This procedure is discussed further in Chapter 2.

1.3.4 Ellipsoidal Shells under Internal Pressure

Ellipsoidal heads of all sizes and shapes are used in the ASME code as end closure for pressure components. The general configuration is shown in Figure 1.11.

Small-size heads are formed by using dyes shaped to a true ellipse. However, large diameter heads formed from plate segments are in the shapes of spherical and torispherical geometries that simulate ellipses as shown in Figures 1.12 and 1.13. Figure 1.12 shows an ASME

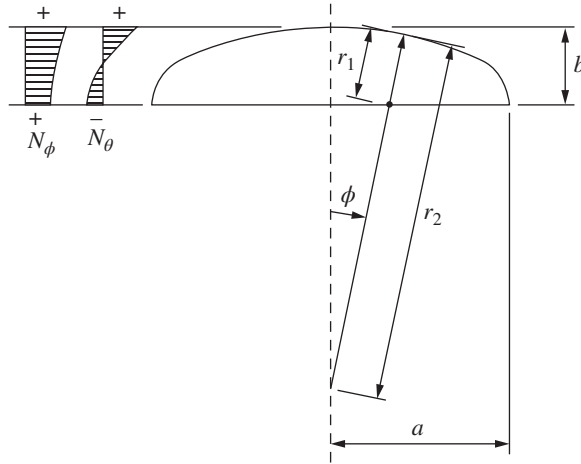


Figure 1.11 Ellipsoidal head under internal pressure

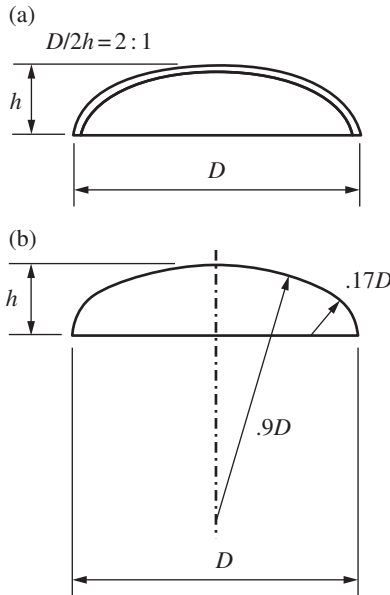


Figure 1.12 2 : 1 elliptical head: (a) exact configuration and (b) approximate configuration

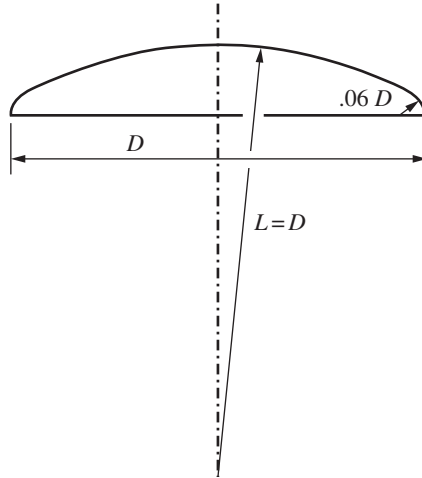


Figure 1.13 Elliptical head with $a/b = 2.96$ ratio

equivalent 2 : 1 ellipsoidal head. It consists of a spherical segment with $R = 0.9D$ and a knuckle with $r = 0.17D$ where D is the base diameter of the head. Figure 1.13 shows a shallow head (2.96 : 1 ratio) referred to as flanged and dished (F&D) head consisting of a spherical segment with $R = D$ and a knuckle section with $r = 0.06D$.

For internal pressure we define $p_r = p$ and $p_\phi = 0$. Then from Eqs. (1.1) and (1.10),

$$N_\phi = \frac{1}{r_2 \sin^2 \phi} (p[r dr + C])$$

$$N_\phi = \frac{1}{r_2 \sin^2 \phi} \left(\frac{pr^2}{2} + C \right). \quad (1.15)$$

The constant C is obtained from the following boundary condition:

$$\text{At } \phi = \frac{\pi}{2}, \quad r_2 = r \quad \text{and} \quad N_\phi = \frac{pr}{2}.$$

Hence, from Eq. (1.15) we get $C = 0$ and N_ϕ can be expressed as

$$N_\phi = \frac{pr^2}{2r_2 \sin^2 \phi}$$

or

$$N_\phi = \frac{pr_2}{2}. \quad (1.16)$$

From Eq. (1.9),

$$N_{\theta} = pr_2 \left(1 - \frac{r_2}{2r_1} \right). \quad (1.17)$$

From analytical geometry, the relationship between the major and minor axes of an ellipse and r_1 and r_2 is given by

$$r_1 = \frac{a^2 b^2}{(a^2 \sin^2 \phi + b^2 \cos^2 \phi)^{3/2}}$$

$$r_2 = \frac{a^2}{(a^2 \sin^2 \phi + b^2 \cos^2 \phi)^{1/2}}.$$

Substituting these expressions into Eqs. (1.16) and (1.17) gives the following expressions for membrane forces in ellipsoidal shells due to internal pressure:

$$N_{\phi} = \frac{pa^2}{2} \frac{1}{(a^2 \sin^2 \phi + b^2 \cos^2 \phi)^{1/2}} \quad (1.18)$$

$$N_{\theta} = \frac{pa^2}{2b^2} \frac{b^2 - (a^2 - b^2) \sin^2 \phi}{(a^2 \sin^2 \phi + b^2 \cos^2 \phi)^{1/2}}. \quad (1.19)$$

The maximum tensile force in an ellipsoidal head is at the apex as shown in Figure 1.11. The maximum value is obtained from Eqs. (1.18) and (1.19) by letting $\phi = 0$. This gives

$$N_{\phi} = N_{\theta} = \frac{Pa^2}{2b} \quad (1.20)$$

For a 2 : 1 head with $a/b = 2$ and $a = D/2$, Eq. (1.18) becomes

$$N_{\phi} = N_{\theta} = 0.5PD \quad (1.21)$$

where D is the base diameter. Comparing this equation with Eq. (1.13) for spherical heads shows that the force, and thus the stress, in a 2 : 1 ellipsoidal head is twice that of a spherical head having the same base diameter.

For an F&D head with $a/b = 2.96$ and $a = D/2$, Eq. (1.18) becomes

$$N_{\phi} = N_{\theta} = 0.74PD \quad (1.22)$$

Comparing this equation with Eq. (1.13) for spherical heads shows the stress of a 2.95 : 1 F&D head at the apex is 2.96 times that of a spherical head having the same base diameter.

A plot of Eqs. (1.18) and (1.19) is shown in Figure 1.11. Equation (1.18) for the longitudinal force, N_{ϕ} , is always in tension regardless of the a/b ratio. Equation (1.19) for N_{θ} on the other hand gives compressive circumferential forces near the equator when the value $a/b \geq \sqrt{2}$.

For large a/b ratios under internal pressure, the compressive circumferential force tends to increase in magnitude, whereas instability may occur for large a/t ratios. This extreme care must be exercised by the engineer to avoid buckling failure. The ASME code contains design rules that take into account the instability of shallow ellipsoidal shells due to internal pressure as described in Chapter 5.

Example 1.4

Determine the required thickness of a 2 : 1 ellipsoidal head with $a = 30$ inches, $b = 15$ inches, and $P = 500$ psi, and allowable stress in tension is $S = 20,000$ psi.

Solution

At the apex, $\phi = 0$, and from Eqs. (1.18) and (1.19),

$$N_\phi = Pa \quad \text{and} \quad N_\theta = Pa$$

At the equator, $\phi = 90^\circ$, and from Eqs. (1.18) and (1.19),

$$N_\phi = \frac{Pa}{2} \quad \text{and} \quad N_\theta = -Pa$$

Thus, the required thickness is $t = Pa/S = 500(30)/20,000 = 0.75$ inch.

Notice at the equator, N_θ is compressive and may result in instability as discussed in Chapter 5.

1.4 Conical Shells

Equations (1.9) and (1.10) cannot readily be used for analyzing conical shells because the angle ϕ in a conical shell is constant. Hence, the two equations have to be modified accordingly. Referring to Figure 1.14, it can be shown that

$$\left. \begin{aligned} \phi = \beta = \text{constant} \\ r_1 = \infty \quad r_2 = s \tan \alpha \quad r = s \sin \alpha \\ N_\phi = N_s. \end{aligned} \right\} \quad (1.23)$$

Equation (1.9) can be written as

$$\frac{N_s}{r_1} + \frac{N_\theta}{s \tan \alpha} = p_r$$

or since $r_1 = \infty$,

$$\left. \begin{aligned} N_\theta &= p_r s \tan \alpha \\ &= p_r r_2 \\ N_\theta &= \frac{p_r r}{\cos \alpha} \end{aligned} \right\} \quad (1.24)$$

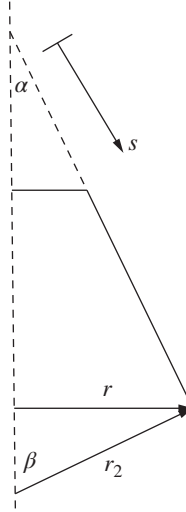


Figure 1.14 Conical shell

Similarly from Eqs. (1.1) and (1.7),

$$\frac{d}{ds}r_1(s \sin \alpha N_s) - r_1 N_\theta \sin \alpha = -p_s s \sin \alpha r_1.$$

Substituting Eq. (1.24) into this equation results in

$$N_s = \frac{-1}{s} \left[\int (p_s - p_r \tan \alpha) s ds + C \right]. \quad (1.25)$$

It is of interest to note that while N_θ is a function of N_ϕ for shells with double curvature, it is independent of N_ϕ for conical shells as shown in Eqs. (1.24) and (1.25). Also, as α approaches 0° , Eq. (1.25) becomes

$$N_\theta = p_r r_2,$$

which is the expression for the circumferential hoop force in a cylindrical shell.

The analysis of conical shells consists of solving the forces in Eqs. (1.24) and (1.25) for any given loading condition. The thickness is then determined from the maximum forces and a given allowable stress.

Equations (1.24) and (1.25) and Figure 1.15 will be used to determine forces in a conical shell due to internal pressure.

From Eq. (1.24), the maximum N_θ occurs at the large end of the cone and is given by

$$N_\theta = p \left(\frac{r_o}{\sin \alpha} \right) \tan \alpha = \frac{p r_o}{\cos \alpha}. \quad (1.26)$$

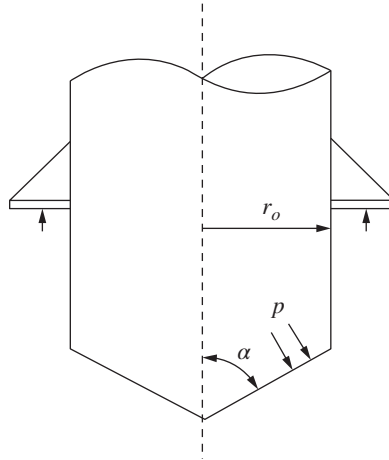


Figure 1.15 Conical bottom head

From Eq. (1.25),

$$\begin{aligned}
 N_s &= \frac{-1}{s} \left(\int -p \tan \alpha s ds + C \right) \\
 &= \frac{-1}{s} \left(-p \tan \alpha \frac{s^2}{2} + C \right). \\
 \text{At } s=L, \quad N_s &= \frac{pr_o}{2} \frac{1}{\cos \alpha}
 \end{aligned} \tag{1.27}$$

Substituting this expression into Eq. (1.27), and using the relationships of Eq. (1.23), gives $C=0$. Equation (1.27) becomes

$$\begin{aligned}
 N_s &= \frac{pr}{2 \cos \alpha} \\
 \text{and max } N_s &= \frac{pr_o}{2 \cos \alpha}.
 \end{aligned} \tag{1.28}$$

It is of interest to note that the longitudinal and hoop forces are identical to those of a cylinder with equivalent radius of $r_o/\cos \alpha$.

All sections of the ASME code have equations for designing conical sections based on Eqs. (1.26) and (1.28).

1.5 Cylindrical Shells

Equipment consisting of cylindrical shells subjected to pressure and axial loads are frequently encountered in refineries and chemical plants. If the radius of the shell is designated by R , Figure 1.16a, then from Figure 1.3 $r_1 = \infty$, $\phi = 90^\circ$, $P = p_r$, and $r = r_2 = R$. The value of the

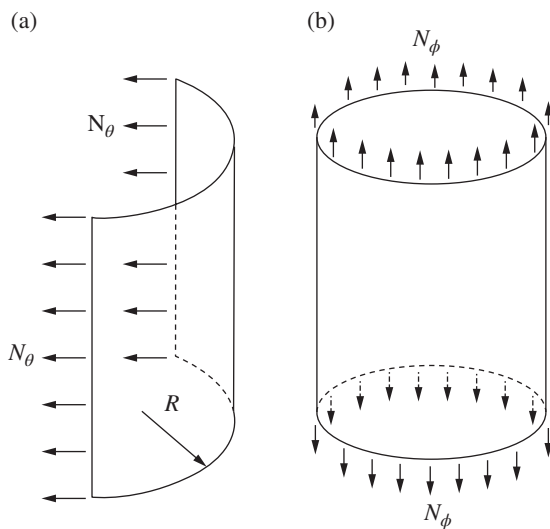


Figure 1.16 Cylindrical shell: (a) circumferential force and (b) longitudinal force

circumferential force N_θ can be obtained by equating the pressure acting on the cross section, Figure 1.16a, to the forces in the material at the cross section. This results in

$$N_\theta = p_r R \tag{1.29}$$

The required thickness, t , of a cylindrical shell due to internal pressure is obtained from Eq. (1.29) as

$$t = \frac{PR}{S} \tag{1.30}$$

where S is the allowable stress and t is the thickness.

The required thickness of cylindrical shells in the ASME code is obtained from a modified Eq. (1.30) that takes into consideration stress variation in the wall of the cylinder for small R/t ratios. This equation is described in Chapter 3.

Similarly, the value of the axial force N_ϕ is obtained by equating the pressure acting on the cross section, Figure 1.16b, to the forces in the material at the cross section. This yields

$$N_\phi = \frac{p_r R}{2} \tag{1.31}$$

The corresponding stress and thickness are obtained from Eq. (1.31) as

$$t = \frac{PR}{2S} \tag{1.32}$$